Novel Influenza A (H1N1) Virus Infection in Children: Chest Radiographic and CT Evaluation

Min Jeong Choi, MD[1]
Young Seok Lee, MD[1]
Jee Young Lee, MD[1]
Kun Song Lee, MD[2]

Departments of [1]Diagnostic Radiology
and [2]Pediatrics, Dankook University
College of Medicine, Dankook University
Hospital, Chungnam 330-715, Korea

Corresponding author:
Young Seok Lee, MD, Department of
Diagnostic Radiology, College of
Medicine, Dankook University, 29 Anseo-
dong, Namdong-gu, Cheonan-si,
Chungnam 330-715, Korea.
Tel. (8241) 550-3955
Fax. (8241) 552-9674
e-mail: yslee@dkuh.co.kr

Objective: The purpose of this study was to evaluate the chest radiographic and CT findings of novel influenza A (H1N1) virus infection in children, the population that is more vulnerable to respiratory infection than adults.

Materials and Methods: The study population comprised 410 children who were diagnosed with an H1N1 infection from August 24, 2009 to November 11, 2009 and underwent chest radiography at Dankook University Hospital in Korea. Six of these patients also underwent chest CT. The initial chest radiographs were classified as normal or abnormal. The abnormal chest radiographs and high resolution CT scans were assessed for the pattern and distribution of parenchymal lesions, and the presence of complications such as atelectasis, pleural effusion, and pneumomediastinum.

Results: The initial chest radiograph was normal in 384 of 410 (94%) patients and abnormal in 26 of 410 (6%) patients. Parenchymal abnormalities seen on the initial chest radiographs included prominent peribronchial marking (25 of 26, 96%), consolidation (22 of 26, 85%), and ground-glass opacities without consolidation (2 of 26, 8%). The involvement was usually bilateral (19 of 26, 73%) with the lower lung zone predominance (22 of 26, 85%). Atelectasis was observed in 12 (46%) and pleural effusion in 11 (42%) patients. CT (n = 6) scans showed peribronchovascular interstitial thickening (n = 6), ground-glass opacities (n = 5), centrilobular nodules (n = 4), consolidation (n = 3), mediastinal lymph node enlargement (n = 5), pleural effusion (n = 3), and pneumomediastinum (n = 3).

Conclusion: Abnormal chest radiographs were uncommon in children with a swine-origin influenza A (H1N1) virus (S-OIV) infection. In children, H1N1 virus infection can be included in the differential diagnosis, when chest radiographs and CT scans show prominent peribronchial markings and ill-defined patchy consolidation with mediastinal lymph node enlargement, pleural effusion and pneumomediastinum.

I n March 2009, there was an outbreak of respiratory disease of unknown origin in Mexico, which was identified in April 2009 as novel influenza A (H1N1) (swine-origin influenza A; S-OIV) (1). The H1N1 virus has been spreading rapidly internationally, and the World Health Organization (WHO) has raised its alert status this outbreak to Phase 6, the pandemic phase (2, 3). In Korea, H1N1 has spread nationwide since the first case was reported in May 2009. Cases were expected to increase significantly during the fall season. However, in August 2010, WHO announced that the H1N1 influenza virus has moved into the post-pandemic period (3).

Although H1N1 has been associated with a self-limited course of mild upper respira-

tory illness, it can also cause severe lower respiratory illness and death (1, 4, 5). Perez-Padilla et al. (1) reported that the risk factors for severe H1N1 illness were still unclear; however, a significant number of affected patients have been young to middle-aged with no specific medical history. Young children are more susceptible to respiratory infection than adults, which make them more vulnerable to severe complications that are occasionally life threatening (6). Therefore, it is important to diagnose the pneumonia associated with H1N1 and to predict the complications and course of illness in children.

In the study presented here, the chest radiographs and CT scans of children with H1N1 virus infections were reviewed to determine the patterns of the infections affecting the lungs.

MATERIALS AND METHODS

Study Population

This study was approved by the institutional clinical research ethics board. Patient informed consents were not required for this retrospective analysis.

From August 24 through November 11, 2009, at Dankook University Hospital in Korea, a total of 925 patients less than 18 years of age were confirmed to have novel influenza A (H1N1) infections; 410 (44%) of these patients received chest radiographs (6 patients also had a chest CT) and were enrolled in the study. The patients included 251 boys and 159 girls. The mean age of the patients was 9.8 years, and the youngest patient was a 2-month-old girl. Twelve patients (3%) were less than 12 months old, 12 patients (3%) were between 13 and 24 months old, 75 patients (18%) were preschool age (between 2 and 5 years of age), 127 patients (31%) were school-age (between 6 and 10 years of age), and the remaining 184 patients (45%) were adolescents (between 11 and 18 years of age).

The clinical signs and symptoms at the time of presentation included fever (n = 401, 98%), cough (n = 389, 95%), rhinorrhea (n = 175, 43%), sore throat (n = 124, 30%), headache (n = 58, 14%), dyspnea (n = 36, 9%), chest pain (n = 24, 6%), vomiting (n = 14, 3%), and diarrhea (n = 13, 3%). All patients were treated with oseltamivir immediately after the results of real-time reverse transcriptase polymerase chain reaction (RT-PCR) of nasal swabs or aspirates were found to be positive for H1N1. Thirty eight (9%) patients were hospitalized in the isolation ward; of these, 12 (3%) patients were hospitalized for severe acute tonsillitis or acute nasopharyngitis and showed normal chest radiographs, and the remaining 26 (6%) patients showed abnormal chest radiographs. All 38 hospitalized

patients were evaluated for super-infections, i.e., other respiratory virus infections (20 of 38 patients were evaluated), mycoplasma PCR and antimycoplasma antibody (19 of 38 were evaluated), and blood cultures for aerobic and anaerobic bacteria (32 of 38 were evaluated). Other respiratory virus infections, identified in the sputum of five patients, included parainfluenza 3 and rhinovirus. There were no combined mycoplasma infections, and all blood cultures were negative. One patient manifested clinically with acute respiratory distress syndrome and required mechanical ventilation in isolation in the intensive care unit for three days. All patients in this study recovered and were discharged from the hospital; there were no deaths. The duration of hospital stays ranged from 2 to 9 days (mean duration, 5.2 days).

Radiography and CT

The indications prompting the initial chest radiographs were severe or unusual manifestations of clinical signs or presentation of abnormal lung sounds on auscultation of the chest. The chest radiographs were performed using computed (CR 900, Kodak, Rochester, NY) and digital radiography equipment (digital DIAGNOST, Philips Medical Systems, Best, The Netherlands). The initial chest radiographs were obtained within three days of the onset of fever, except in two patients who delayed visiting the hospital. In 26 patients hospitalized for pneumonia, follow-up chest radiographs were obtained during their hospitalization and after discharge. Twenty-two patients had follow-up chest radiographs within two days after the initial chest radiograph. The remaining four patients also underwent the second examination within five days after the initial chest radiograph.

The high-resolution CT (HRCT) was obtained based on

Table 1. Initial Radiographic Findings of Novel Influenza A (H1N1) Virus Infection in Children

| Radiographic Findings	n = 410
Normal initial chest radiograph	384 (94%)
Abnormal initial chest radiograph	26 (6%)
Prominent peribronchial marking	25/26
Consolidation + ground-glass opacity	22/26
Lobar	0
Non-lobar	22
Ground-glass opacity without consolidation	2/26
Consolidation without ground-glass opacity	0/26
Atelectasis	12/26
Lobar	3
Non-lobar	9
Pleural effusion	11/26
Pneumomediastinum	1/26

the judgment of the pediatrician in six cases. The indications for the HRCT were progressing and more severe clinical signs or symptoms, worsened imaging findings on follow-up chest radiographs, and inconsistent clinical symptoms and radiological findings. The HRCT was performed on a 64-MDCT scanner (LightSpeed VCT, GE Healthcare, Milwaukee, WI). The HRCT was obtained using the pediatric low-dose protocol without contrast enhancement, 120 kV, 60 mAs, and reconstruction of 0.625 mm intervals. The images were viewed on both the lung (window width, 1500 HU; level, −700 HU) and mediastinal (window width, 350 HU; level, 20 HU) settings.

Two patients underwent chest CT on the same day the initial radiographs were performed. The other four patients had their chest CT within five days of the initial chest radiograph.

Image Interpretation

Two experienced radiologists reviewed the chest radiographs and CT scans retrospectively and agreed on the findings in consensus. All images were reviewed on a PACS workstation.

The initial chest radiographs were classified as normal or abnormal. One abnormal radiograph (in a 6-month-old male patient with a ventricular septal defect) was initially

A

B

C
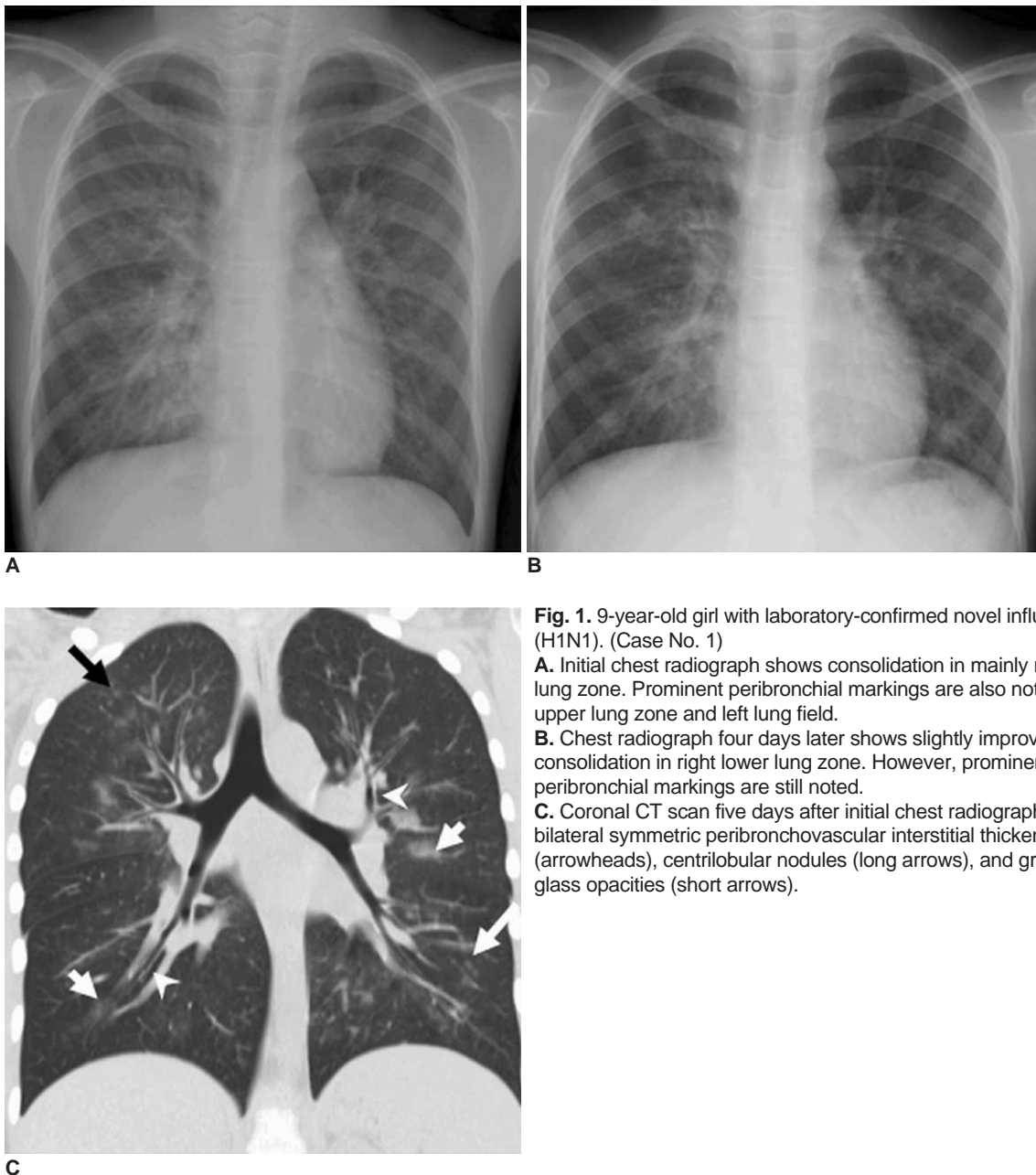
Fig. 1. 9-year-old girl with laboratory-confirmed novel influenza A (H1N1). (Case No. 1)
A. Initial chest radiograph shows consolidation in mainly right lower lung zone. Prominent peribronchial markings are also noted in right upper lung zone and left lung field.
B. Chest radiograph four days later shows slightly improved consolidation in right lower lung zone. However, prominent peribronchial markings are still noted.
C. Coronal CT scan five days after initial chest radiograph shows bilateral symmetric peribronchovascular interstitial thickening (arrowheads), centrilobular nodules (long arrows), and ground-glass opacities (short arrows).

reported to be normal; the radiographic findings (increased peripheral pulmonary vascularity due to underlying left-to-right shunt) in this case were thought to be consistent with pre-existing findings on previous radiographs. The parenchymal abnormalities were further assessed for peribronchial markings (tramline shadow or peribronchovascular cuffing), consolidation (homogeneous opacity with obscuration of pulmonary vascular structures), and ground-glass opacities (increased opacity without obscuration of pulmonary vascular structures). Consolidation was divided into lobar and non-lobar containing segmental or subsegmental regions of the lungs. The involvement was categorized as unilateral or bilateral. In addition, the predominant distribution was characterized as being in the upper, middle, or lower lung zones (each comprising a

third of the craniocaudal extent of the lung fields on frontal radiographs). The radiographs were assessed for the presence of atelectasis, pleural effusion, pneumomediastinum, and other complications.

The HRCT was evaluated for the pattern and distribution of lung parenchymal lesions:, including peribronchovascular interstitial thickening (correlated with prominent peribronchial markings on radiographs), centrilobular nodules, ground-glass opacities, and consolidations. All additional findings were recorded and these included the presence of mediastinal lymph nodes (right paratracheal > 9 mm, hilar > 6.5 mm in short diameter, and any visible lymph nodes at other sites) (7), as well as other complications such as pleural effusions, atelectasis, pneumomediastinum, and pneumothorax.

A

B

C
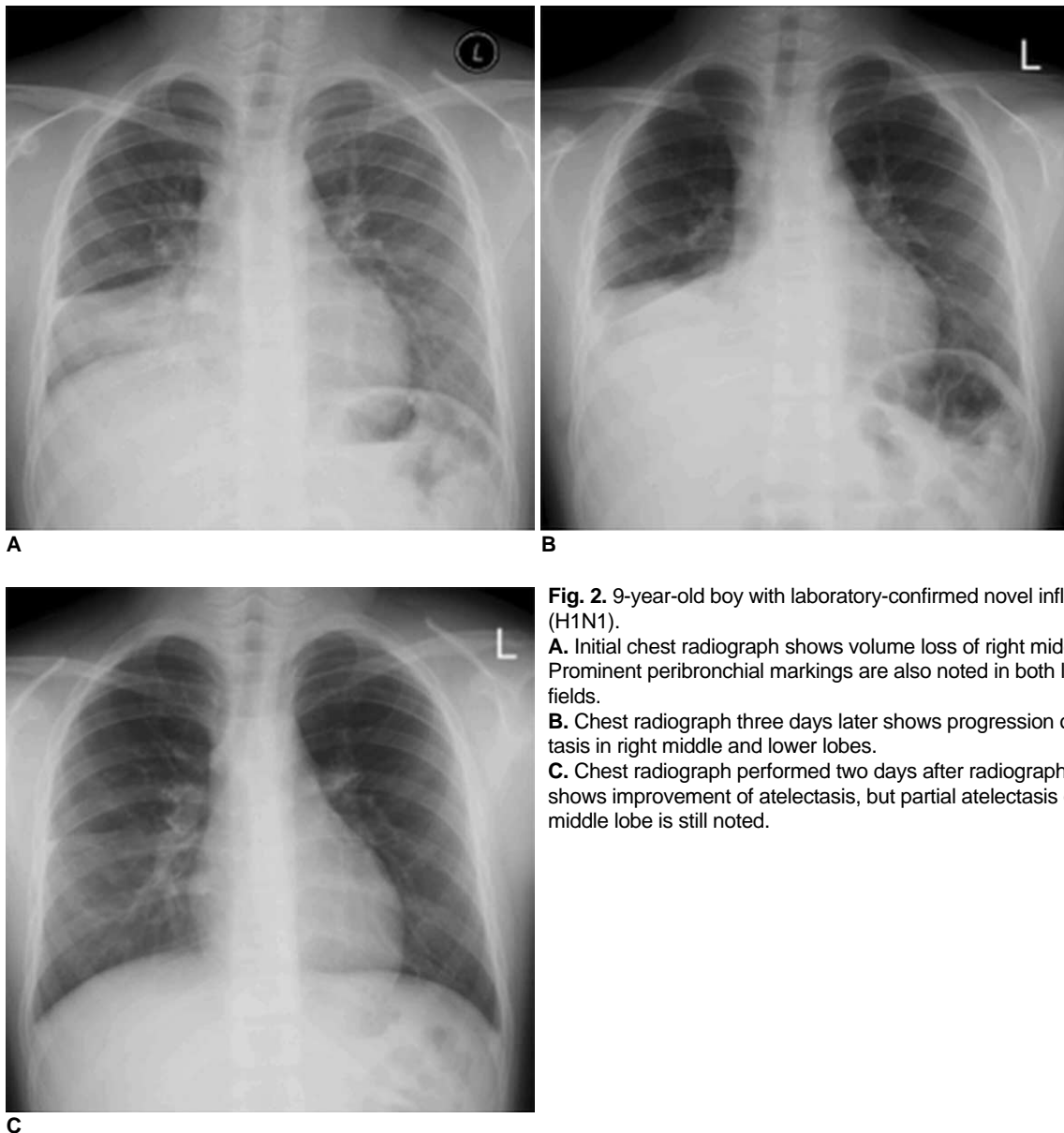
Fig. 2. 9-year-old boy with laboratory-confirmed novel influenza A (H1N1).
A. Initial chest radiograph shows volume loss of right middle lobe. Prominent peribronchial markings are also noted in both lung fields.
B. Chest radiograph three days later shows progression of atelectasis in right middle and lower lobes.
C. Chest radiograph performed two days after radiograph in **B** shows improvement of atelectasis, but partial atelectasis of right middle lobe is still noted.

RESULTS

The initial chest radiograph was normal in 384 of 410 (94%) patients and abnormal in 26 of 410 (6%) patients.

The imaging abnormalities identified in the initial radiographs are summarized in Table 1. Prominent peribronchial markings, present in 25 (96%) patients, and consolidation, present in 22 (85%) patients, were the

Table 2. CT Findings of Novel Influenza A (H1N1) Virus Infection in Children

Case No.	Age (years)	Sex	CT Findings			
			Distribution	Patterns	Mediastinal Lymph Node	Complication
1	9	F	Bilateral, symmetric No predominant lobe	Peribronchovascular interstitial thickening, Centrilobular nodules, GGO	None	None
2	16	M	Unilateral (Lt) Lower lobe predominance	Peribronchovascular interstitial thickening, Centrilobular nodules, GGO Consolidation,	Rt. paratracheal Paraaortic	Pneumomediastinum
3	17	M	Unilateral (Rt) Lower lobe predominance	Peribronchovascular interstitial thickening, Centrilobular nodules	Rt. paratracheal	Pneumomediastinum
4	8	F	Unilateral (Lt) Lower lobe predominance	Peribronchovascular interstitial thickening, Centrilobular nodules, GGO	Rt. paratracheal	Pleural effusion (Lt)
5	6	M	Bilateral (Rt < Lt) Upper and middle lobe predominance	Peribronchovascular interstitial thickening, Consolidation, GGO	Rt. paratracheal	Pleural effusion (Lt), Pneumomediastinum, Subsegmental atelectasis
6	9	M	Unilateral (Rt) Lower lobe predominance	Peribronchovascular interstitial thickening, Consolidation, GGO	Rt. paratracheal	Pleural effusion (Rt)

Note.— GGO = ground-glass opacity, Lt = left, No. = number, Rt = right
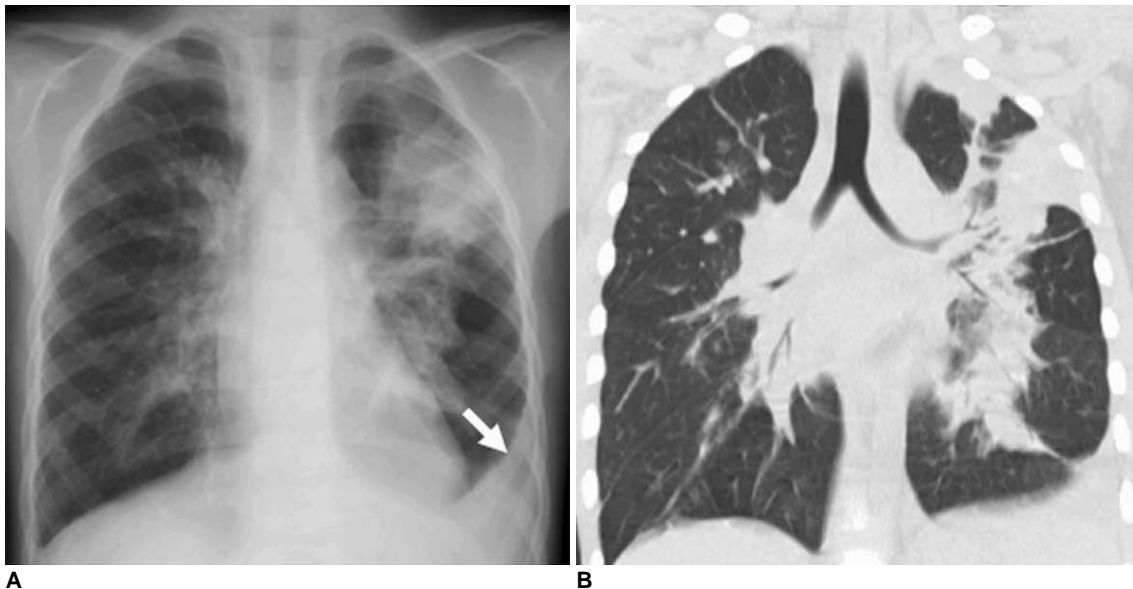
Fig. 3. 6-year-old boy with laboratory-confirmed novel influenza A (H1N1). (Case No. 5)
A. Initial chest radiograph shows consolidations in left upper and both middle lung zones. Prominent peribronchial markings are noted in right lung field. Pleural effusion (arrow) is also noted in left costophrenic angle.
**B.** Coronal CT scan one day after initial chest radiograph shows bilateral peribronchial consolidations, which are predominant in left lung field.

major findings (Fig. 1). In all of the 22 cases with consolidations, the consolidation was associated with ground-glass opacities. The distribution and pattern of the consolidation was non-lobar and ill-defined patchy areas of the lung. Only two patients (8%) had ground-glass opacities without consolidation and no patient had consolidation without ground-glass opacities. Atelectasis was noted in 12 of 26 (46%) patients (Fig. 2), three of these cases were lobar, and nine were non-lobar. A pleural effusion was detected in 11 of 26 (42%) patients. A pneumomediastinum was detected in only one case on the initial radiographs, and a pneumothorax was not detected in any of the cases. The involvement of parenchymal lesions was bilateral in 19 of 26 (73%) cases, eight of which were symmetric and the remaining 11 showed asymmetric bilateral involvement. By contrast, unilateral involvement was noted in 7 of 26 (27%) patients.

The lung abnormalities were commonly found in the
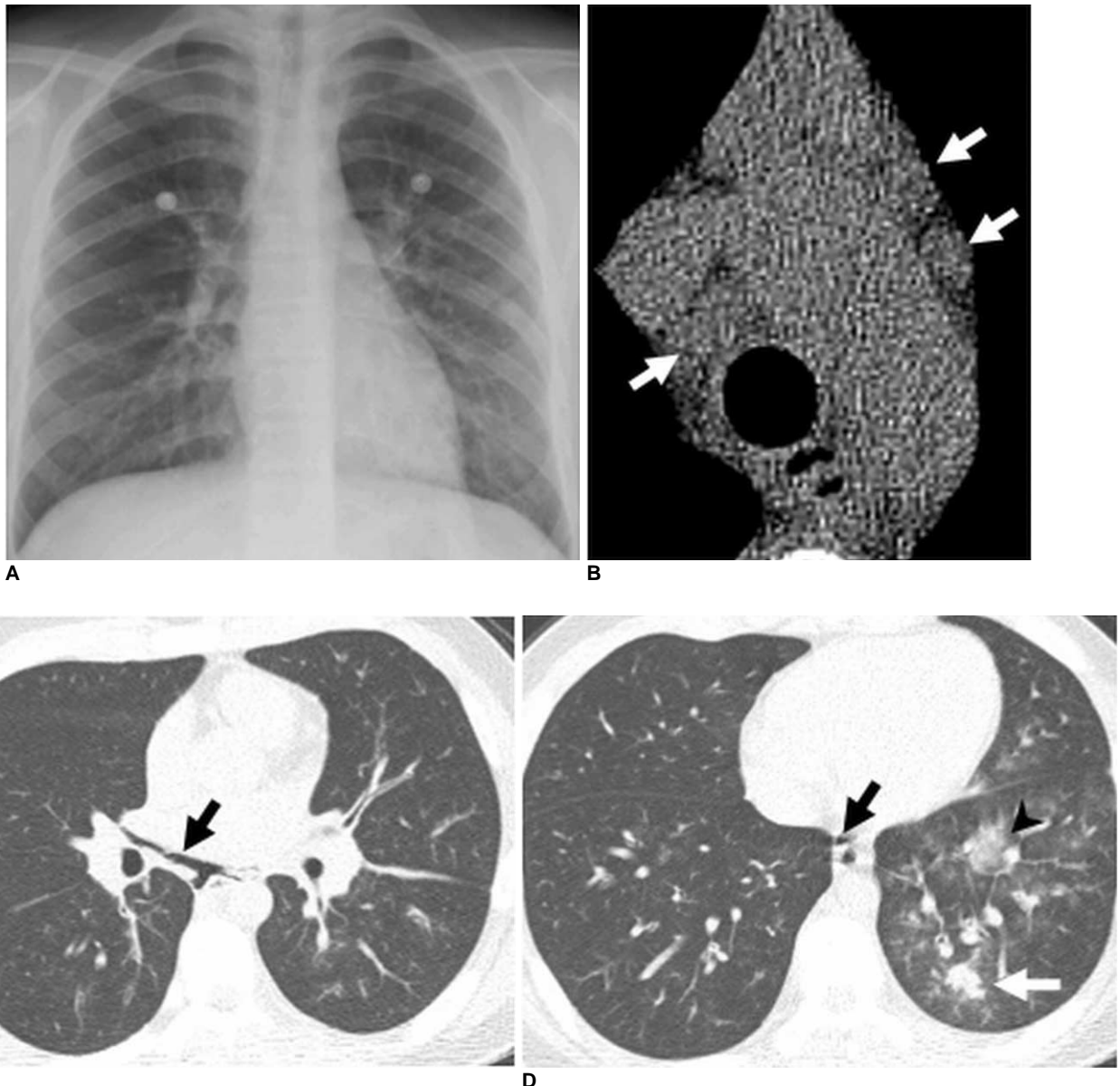
Fig. 4. 16-year-old boy with laboratory-confirmed novel influenza A (H1N1). (Case No. 2)
A. Initial radiograph shows focal area of consolidation in left retrocardiac area. Prominent peribronchial markings are also seen in right lower lung zone and left lung fields.
B. Magnified view of mediastinum on CT scan on same day shows several lymph nodes at right paratracheal and paraaortic nodal stations (arrows).
C. High-resolution CT scan at level of left atrium shows pneumomediastinum (arrow) which was not seen on chest radiograph.
D. High-resolution CT scan caudal to **C** shows ill-defined centrilobular nodules, ground-glass opacities (arrowhead), and focal area of consolidation (white arrow) mainly in left lower lobe. Pneumomediastinum (black arrow) is also noted.

lower lung zone (22 of 26, 85%), and were distributed among the lower lung zone alone (14 of 26, 54%), the middle/lower lung zone (7 of 26, 27%) and the upper/lower lung zone (1 of 26, 4%). In two patients, the distribution of lung abnormalities was diffuse without zonal predominance (2 of 26, 8%).

As shown on serial radiographs, the lung abnormalities began to improve in one day (5 of 26, 19%) or in two days (7 of 26, 27%). The remaining 14 patients (54%) also showed improvement on the follow-up radiographs within one week. Among the 26 patients, six showed temporary worsening on early follow-up radiographs; however, there was no continuous deterioration observed. Mixed features of focal improvement and focal aggravation were noted in two patients, but they also showed improvement of the lung abnormalities within one week.

High-resolution CT scans were performed in six patients (Table 2). On the HRCTs, lung parenchymal lesions consisted of peribronchovascular interstitial thickening (n = 6) (Fig. 1), multifocal ground-glass opacities (n = 5), centrilobular nodules (n = 4), and ill-defined patchy consolidations (n = 3) (Figs. 3, 4). The distribution of lesions was bilateral and symmetric (Fig. 1) in one patient, the remaining five patients showed unilateral (n = 4) or asymmetric bilateral (n = 1) involvement. Mediastinal lymph nodes were detected in five patients (Fig. 4). These patients had lymph nodes > 9 mm at the right paratracheal nodal station and one also had two 7 mm lymph nodes at the paraaortic nodal station. Pleural effusion was noted in half of the patients (n = 3). Although only one radiograph showed pneumomediastinum, three out of six chest CT scans revealed a pneumomediastinum (Fig. 4).

DISCUSSION

Influenza virus belongs to the family Orthoparamyxoviridae and is a single-stranded RNA virus. Influenza is classified into A, B, and C types. Influenza A is further classified into 16HA subtypes and 9NA subtypes on the basis of the antigenicity of its hemagglutinin and neuraminidase molecules (2, 8). The novel influenza A (H1N1) probably is a new strain that resulted from the reassortment of recent North American H3N2 and H1N2 (avian/human/swine 'triple' reassortant virus) with Eurasian avian-like swine viruses (2).

Influenza virus usually causes an upper respiratory infection in children and young adults. However it can sometimes cause a lower respiratory tract infection such as bronchitis, bronchiolitis, and pneumonia (6, 9). Similar to seasonal influenza, the novel influenza A (H1N1) is also transmitted by respiratory droplets and the most common

clinical manifestations include fever, cough, sore throat, dyspnea, and respiratory distress (1). Although the recent pandemic of H1N1 infection has usually been associated with mild upper respiratory illness and a self limited course of disease, it can also cause severe lower respiratory illness and death (1, 4, 5).

Histologically, the influenza virus proliferates on the surface of respiratory mucosa and the airway walls become congested with associated infiltration of mononuclear cells. Epithelial cells are degenerated and desquamated and parenchymal changes show typical features of diffuse alveolar damage (10).

Perez-Padilla et al. (1) evaluated the clinical and epidemiological characteristics of persons hospitalized for pneumonia caused by novel influenza A (H1N1) and reported that their study patients showed bilateral patchy alveolar opacities on radiographs. Agarwal et al. (11) evaluated chest imaging findings in patients with H1N1 virus infection and reported that even though the chest radiographs were normal in more than half of the patients, the infection progressed to bilateral extensive air-space disease with lower and central lung predominance. Furthermore, a recent study (12) focusing on children reported that while 67% of the initial chest radiographs in children with a mild and self-limited clinical course of H1N1 infection were normal (compared with the 94% rate of initial radiographs that were normal in our study population), they may demonstrate prominent peribronchial markings with hyperinflation. They also reported that bilateral and multifocal areas of consolidation, often associated with ground-glass opacities, are the predominant radiographic findings in pediatric patients with a more severe clinical course of H1N1 infection (12). When compared with previous studies (1, 11, 12), our study showed similar radiographic findings, including ill-defined patchy and non-lobar consolidation, bilateral involvement, and lower lung zone predominance.

However, there were also differences in radiographic findings. Perez-Padilla et al. (1) reported that linear, reticular or nodular shadows (interstitial opacities) were common; whereas, in the study reported here, these interstitial opacities were not definite in any of the patients. Additionally, Lee et al. (12) have reported that nodular or reticular opacities were not observed in any patients.

The common radiographic manifestations of typical influenza-induced pneumonia include bilateral reticulonodular opacities, which is the pattern of interstitial pneumonia (9, 13). Lee et al. (14) have suggested that radiologists should be aware of the radiographic and CT findings of viral infection in order to promptly diagnose

novel influenza A (H1N1) pneumonia. In their study (14), they suggested that a case showing lobar-distributed consolidation and peripheral ground-glass opacities, which showed positive results for both the pneumococcal urine antigen assay and gram-positive cocci on sputum culture, had combined components of bacterial lobar pneumonia. By contrast, in our study, there were no lobar-distributed consolidations or ground-glass opacities.

Secondary bacterial pneumonia usually presents a pattern consistent with bronchopneumonia, including lobular, subsegmental, or segmental consolidation (13, 15). Song et al. (8) reported that the major radiological findings of childhood lower respiratory tract infections caused by the typical influenza virus were bilateral perihilar, peribronchial infiltration and hyperinflation, but that atelectasis and consolidation are rare. In our study, although one of the most common radiographic abnormalities was the pattern of bronchopneumonia (non-lobar consolidation), there were no positive findings on the work-up for super-infections.

The common findings on CT for typical influenza pneumonia consist of diffuse or multifocal ground-glass opacities and small centrilobular nodules, which may be related to alveolar hemorrhage (9). Tanaka et al. (16) have described high-resolution CT findings of influenza virus pneumonia comprising bilateral ground-glass opacities in a lobular distribution. Mollura et al. (17) evaluated the imaging findings in a fatal case of novel influenza A (H1N1) and reported that the CT showed peripheral ground-glass opacities, suggesting peribronchial injury. Additionally, bilateral multifocal ground-glass opacities, small nodules, and consolidation have been described as the main chest CT findings in previous reports on novel influenza A (H1N1) virus infection (11, 18, 19). On the CT scans in our study population, mediastinal lymph nodes, pleural effusion, and pneumomediastinum were frequently detected. Three patients had pneumomediastinum, which was noted in only one patient on the radiographs.

Other findings in this study included alveolar rupture, pleural effusion, and abnormal mediastinal lymph nodes. The most common cause of pneumomediastinum is rupture of alveoli. Alveolar rupture may occur under conditions of elevated intra-alveolar pressure such as coughing, vomiting, straining, and blunt chest trauma (20–22). In this study, all patients with a pneumomediastinum had a history of a few days of violent coughing, dyspnea, and chest pain. Pleural effusion is rare in typical influenza pneumonia (9). Lee et al. (12) also reported that pleural effusions were not observed in their study population. By contrast, in this study, pleural effusion was frequently detected in both the abnormal initial radiographs and CT

scans. Andronikou (7) reported size criteria for abnormal mediastinal lymph nodes in children. For children over eight years of age, he suggested that right paratracheal lymph nodes > 9 mm and hilar lymph nodes > 6.5 mm were abnormal. Any visible lymph nodes at other sites were also considered abnormal, independent of their size (7). By these criteria, five patients had abnormal mediastinal lymph nodes.

Limitations to this study include a small study population, making generalization of the imaging features of H1N1 infection in children difficult. Additionally, there was an interval between the initial chest radiograph and CT, so CT findings cannot be completely correlated with radiographic findings. Further, examinations to detect super-infections were not extensive, respiratory infections in addition to H1N1 were detected in some patients, and examination of the mediastinal lymph nodes was limited to only non-contrast CT scans.

In conclusion, the results of this study showed that abnormal chest radiographs were uncommon in children with novel swine-origin influenza A (H1N1) virus (S-OIV) infection. In children, H1N1 virus infection can be included in the differential diagnosis, when chest radiographs and CT scans show prominent peribronchial markings and ill-defined patchy consolidation with mediastinal lymph node, pleural effusion and pneumomediastinum.

References

1. Perez-Padilla R, de la Rosa-Zamboni D, Ponce de Leon S, Hernandez M, Quiñones-Falconi F, Bautista E, et al. Pneumonia and respiratory failure from swine-origin influenza A (H1N1) in Mexico. *N Engl J Med* 2009;361:680-689
2. Neumann G, Noda T, Kawaoka Y. Emergence and pandemic potential of swine-origin H1N1 influenza virus. *Nature* 2009;459:931-939
3. World Health Organization Website. Global alert and response: current WHO phase of pandemic alert ? update58. www.who.int/csr/disease/avian_influenza/phase/en/index.html. Accessed November 12, 2009
4. Centers for Disease Control and Prevention (CDC) Update: infectious with a swine-origin influenza A (H1N1) virus--United States and other countries, April 28, 2009. *MMWR Morb Mortal Wkly Rep* 2009;58:431-433
5. Update: Swine influenza A(H1N1) infections - California and Texas, April 2009. *MMWR Morb Mortal Wkly Rep* 2009;58:435-437
6. Yun BY, Kim MR, Park JY, Choi EH, Lee HJ, Yun CK. Viral etiology and epidemiology of acute lower respiratory tract infection in Korean children. *Pediatr Infect Dis J* 1995;14:1054-1059
7. Andronikou S. Pathological correlation of CT-detected mediastinal lymphadenopathy in children: the lack of size threshold criteria for abnormality. *Pediatr Radiol* 2002;32:912
8. Song HT, Park CK, Shin HJ, Choi YW, Jeon SC, Hahm CK, et al. Radiologic findings of childhood lower respiratory tract infection by influenza virus. *J Korean Radiol Soc* 2002;47:227-

231

9. Kim EA, Lee KS, Primack SL, Yoon HK, Byun HS, Kim TS, et al. Viral pneumonias in adults: radiologic and pathologic findings. *Radiographics* 2002;22:S137-S149

10. Feldman PS, Cohan MA, Hierholzer WJ Jr. Fatal Hong Kong influenza: a clinical, microbiological and pathological analysis of nine cases. *Yale J Biol Med* 1972;45:49-63

11. Agarwal PP, Cinti S, Kazerooni EA. Chest radiographic and CT findings in novel swine-origin influenza A (H1N1) virus (S-OIV) infection. *AJR Am J Roentgenol* 2009;193:1488-1493

12. Lee EY, McAdam AJ, Chaudry G, Fishman MP, Zurakowski D, Boiselle PM. Swine-origin influenza A (H1N1) viral infection in children: initial chest radiographic findings. *Radiology* 2010;254:934-941

13. Oliveira EC, Marik PE, Colice G. Influenza pneumonia: a descriptive study. *Chest* 2001;119:1717-1723

14. Lee CW, Seo JB, Song JW, Lee HJ, Lee JS, Kim MY, et al. Pulmonary complication of novel influenza A (H1N1) infection: imaging features in two patients. *Korean J Radiol* 2009;10:531-534

15. Khater F, Moorman JP. Complications of influenza. *South Med J* 2003;96:740-743

16. Tanaka N, Matsumoto T, Kuramitsu T, Nakaki H, Ito K, Uchisako H, et al. High resolution CT findings in community-acquired pneumonia. *J Comput Assist Tomogr* 1996;20:600-608

17. Mollura DJ, Asnis DS, Crupi RS, Conetta R, Feigin DS, Bray M, et al. Imaging findings in a fatal case of pandemic swine-origin influenza A (H1N1). *AJR Am J Roentgenol* 2009;193:1500-1503

18. Ajlan AM, Quiney B, Nicolaou S, Müller NL. Swine-origin influenza A (H1N1) viral infection: radiographic and CT findings. *AJR Am J Roentgenol* 2009;193:1494-1499

19. Yun TJ, Kwon GJ, Oh MK, Woo SK, Park SH, Choi SH, et al. Radiological and clinical characteristics of a miliary outbreak of pandemic H1N1 2009 influenza virus infection. *Korean J Radiol* 2010;11:417-424

20. Zylak CM, Standen JR, Barnes GR, Zylak CJ. Pneumomediastinum revisited. *Radiographics* 2000;20:1043-1057

21. Damore DT, Dayan PS. Medical causes of pneumomediastinum in children. *Clin Pediatr (Phila)* 2001;40:87-91

22. Abolnik I, Lossos IS, Breuer R. Spontaneous pneumomediastinum. A report of 25 cases. *Chest* 1991;100:93-95